Contents lists available at ScienceDirect

Nuclear Inst. and Methods in Physics Research, B

The dual ion beam microprobe

Milko Jakšić [a,*], Georgios Provatas [a,*], Iva Božičević Mihalić [a], Andreo Crnjac [a], Donny Cosic [a], Toni Dunatov [a], Oleksandr Romanenko [b], Zdravko Siketić [a]

[a] *Ruđer Bošković Institute, Bijenička cesta 54, 10000 Zagreb, Croatia*
[b] *Nuclear Physics Institute of the Czech Academy of Sciences, 250 68 Řež, Czech Republic*

A B S T R A C T

A new experimental setup for dual ion microbeam irradiation and analysis of materials has been designed and commissioned at the Ruđer Bošković Institute (RBI). Ion beams in the MeV energy range are provided by two tandem accelerators, a 1.0 MV Tandetron and a 6.0 MV EN tandem Van de Graaff. The dual microprobe end station is primarily dedicated for the performance of experiments where one ion microbeam is used for the irradiation, while the other ion microbeam is used for the analysis or 'probing' the *in-situ* changes induced during the target irradiation. Likewise, both microbeams can be also used independently, for experiments involving either ion beam characterization or ion beam irradiation techniques. The ion beam from the small tandem accelerator is focused with a magnetic quadrupole triplet, which is more suitable for the high spatial resolution work with light ions. The ion beam from the larger accelerator is focused by an electrostatic quadruplet that enables easier focusing of heavy ions. Details of the experimental setup, its capabilities in terms of ion beam irradiation and analysis techniques, as well as the first applications, are presented.

1. Introduction

There are many advantages for the *in-situ* investigation of radiation-induced changes in materials, since the irradiated sample characteristics may be altered during the time period between the irradiation and the analysis. In the case of ion beam irradiation, there are setups that enable *in-situ* monitoring of induced changes by other conventional characterization methods that could be introduced into the irradiation chamber. These include imaging techniques such as SEM or TEM [1,2], or other characterization techniques like Raman [3,4], luminescence [5,6] and others. However, examples of setups that enable in situ monitoring radiation induced changes by other ion beam-based techniques are scarce, although there are few (e.g. ion beam analysis – IBA) that can effectively monitor these changes. For example, if irradiation is done on crystalline materials, RBS channelling can provide extremely useful and quantitative result about the induced disorder in crystal lattice. Also, implantation doses can be monitored by IBA techniques such as PIXE, RBS and ERDA, while in terms of degradation of electronic transport properties due to irradiation, IBIC is certainly another very useful and quantitative technique. Unfortunately, all these techniques can be rarely used with a same ion beam as the one used for irradiation. The natural alternative is therefore an experimental setup that enables access of two different ion beams into the same scattering chamber. Such cases are only possible if the ion beams are provided by two different accelerators. There are several arrangements worldwide where multiple ion beams enter the same scattering chamber, but most of them are primarily used for the purpose of dual and triple beam irradiation [7–9]. This approach is today mostly used for simulating high radiation environments, such as those found in fusion reactors [10]. None of these systems is capable to work with focussed ion beams.

At the RBI accelerator facility, which consists of two electrostatic tandem accelerators, there are two positions where ion beams from both accelerators can be directed into the same intercepting point (Fig. 1). The first one is reserved for the DiFU (Dual ion beam for FUsion) scattering chamber, used primarily for dual beam irradiation and which is described elsewhere [11]. The second dual beam scattering chamber, which will be explained in details here, is primarily designed to enable performance of different irradiation techniques and a variety of ion beam characterization techniques, using focused ion beams. Therefore, this end station, named DuMi (Dual Microprobe), is equipped with focusing and scanning systems for both of the ion beams.

When designing the dual microprobe set up, it was particularly important to take into account the fact that the 1.0 MV Tandetron accelerator provides primarily light ions (H, He) accelerated by voltages

between 0.1 and 1.0 MV. For these ions, which are mainly intended for IBA imaging, the most appropriate focusing system would be the one based on magnetic quadrupoles, as high spatial resolution is required. On the other side, for ion beams from the 6.0 MV Tandem Van de Graaff that currently accelerate ions by voltages between 0.5 and 4.0 MV, and which can deliver heavier ions with a range in material similar to those of light ions from the small accelerator, the use of electrostatic focusing lens has significant advantages. For electrostatic focusing systems only ion charge and energy determine the focusing parameters, which simplifies the focusing of heavy ion. Finally, it is important to note that both of the accelerators are providing a variety of ions using negative ion sputtering sources, while for the provision of helium ions, another, dedicated sources using charge exchange are employed.

2. Materials and methods

2.1. Scattering chamber

The basic geometry of the DuMi scattering chamber is primarily determined by the selection of the intercepting point between the two ion beams. As it is seen from the sketch presented in Fig. 1 and Fig. 2, the angle between the beam axes from the two accelerators is 40 degrees. These axes intercept in the centre of the main chamber which is of a cylindrical shape. The central volume of the chamber, hosts the majority of detectors for ion beam analysis, that are aligned to the cross-point, the common focus of both microbeams. In the spaces between the focusing lens and the main chamber there are also two small pre-chambers, where the beam can be focused as well. At these positions, significantly higher demagnification should enable higher microbeam spatial resolution. This may be a significant advantage for applications that can be performed in the small volume of the pre-chamber.

Currently, a 30 mm^2 SDD detector for PIXE is mounted on the top lid of the chamber, viewing the cross-point of the main chamber cylinder from above, under the 60 degree in respect to the horizontal plane. In order to reduce the effect of x-ray absorption, the sample holder can be positioned under and angle of 30 degrees in respect to beam direction, which reduces the angle towards the x-ray detector to only 30 degrees (as it is visible on Fig. 2). Concerning the detection of gamma rays for PIGE, in order to achieve the largest possible solid angle, an intrinsic Ge detector is mounted horizontally under the 90 degrees angle with respect to the beam axis from the 6.0 MV tandem. It is assumed that PIGE will be performed by higher energy range protons, that only the larger accelerator can provide, enabling higher cross sections for gamma ray emission. An annular RBS detector with solid angle of up to 2.5 sr, is

mounted in the direction of the 1.0 MV accelerator, on the rail of 10 cm length, in the tube between the pre-chamber and the main chamber. This detector is oriented towards the long focus position, but can be rotated by 180 degrees, enabling detection of forward scattering events (off-axis STIM) when the short focus position is being used. On the same rail, a beam chopper for the indirect measurements of the beam intensity is positioned as well. The chopper, typically used for applications in high beam current mode, is made with a silicon charged-particle detector that detects backscattering from a rotating vane which periodically intercepts the microbeam. For the low current operation mode (<fA), chopper system can be adopted in a way that pin diode periodically intercepts the beam. Between the target position in the chamber centre and Faraday cup for the beam direction of the 1.0 MV tandem, an interchangeable pin diode of 100 mm^2 is mounted on a linear translator for the performance of direct STIM (only from direction of small tandem) and off-axis STIM. The same diode can be used for the off-axis STIM when the beam from 6.0 MV tandem is being used.

There are two xyz Piezo stages (SmarAct) on which the sample holders are attached and which are used for the precise sample positioning. Both of these stages can be programmed to perform sample scanning. The main stage, positioned in the center of the chamber, can host many samples which have to be positioned within an area (x,y) of 50×80 mm. Positioning of samples mounted on this stage is observed by two cameras, where the coarse one has a field of view of the cm range, while for the fine one the field of view is 5 mm. The fine camera is attached to the Infinity long working distance microscope with a fixed working distance and fixed field of view. The small depth of field of this system, results in decrease of sharpness for small changes in z-axis, enabling the exact positioning of the sample along the z-axis. This is in particular important when working with two microbeams that should intercept in the same xyz position.

The xyz Piezo stage at the 'short' focus position of the pre-chamber (microbeam from the small tandem accelerator), can accept only few and small samples, that can be positioned within an area of 10×30 mm. There are two possibilities for viewing samples at this position, the first one is using a long working distance microscope (view field 2 mm) which is aimed at a mirror that enables viewing the sample surface from the front and under the angle of 20 degrees with respect to the beam axis. The second one is by using another long working distance microscope that can be attached at the position of the Faraday cup, which has to be temporary removed if that microscope is to be used. For the short focus position, the same STIM and off-axis STIM detectors used for long focus position, can be used. Alternatively, earlier explained annular detector used for RBS can be rotated by 180 degrees for the detection of
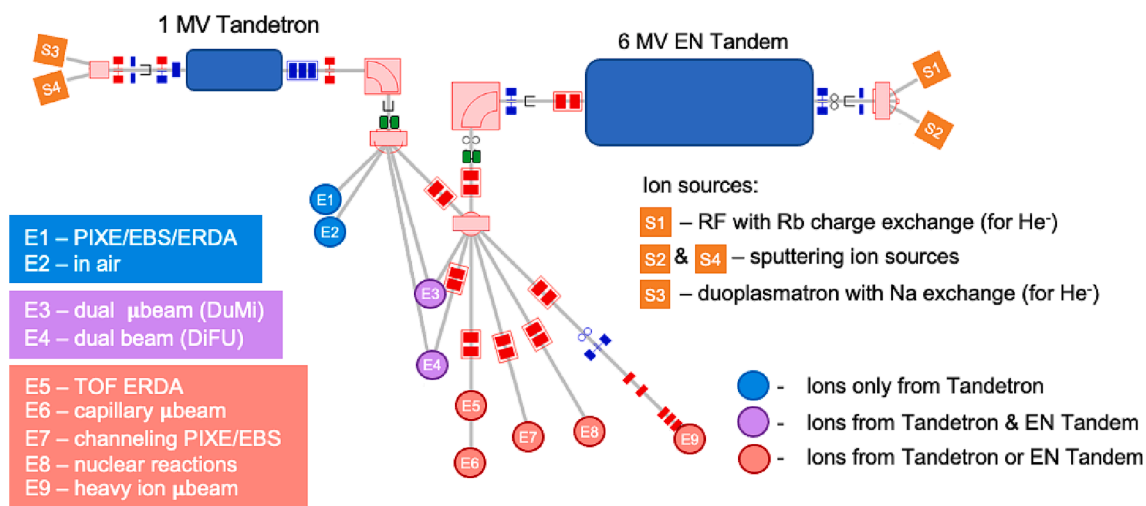

Fig. 1. Layout of the RBI accelerator facility with DuMi end station marked as E3. Green squares indicate positions of the object slits. DiFU end station is marked as E4.
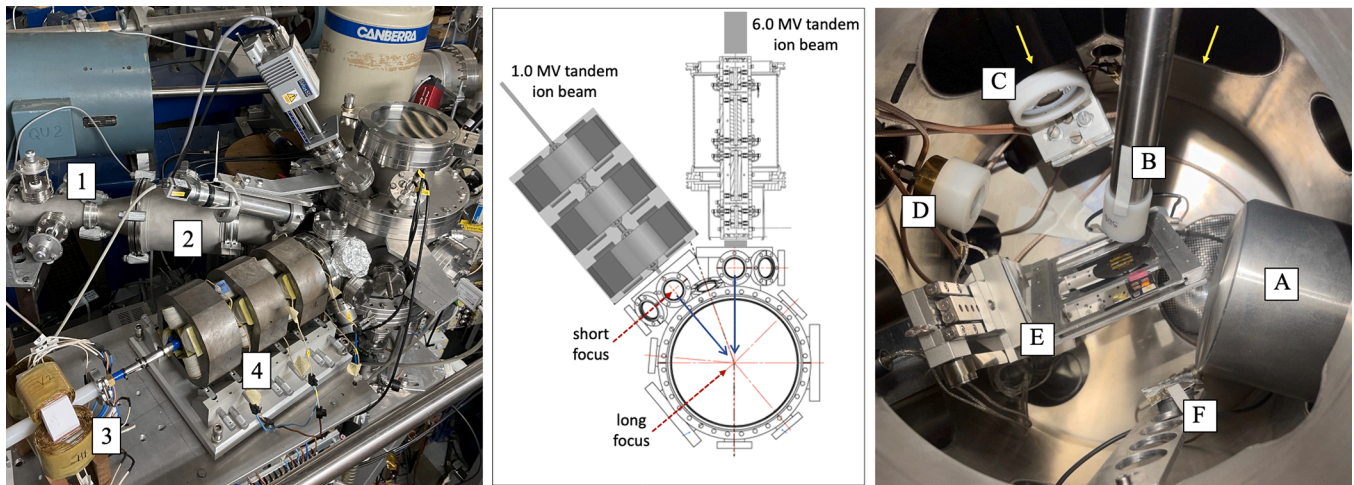
Fig. 2. Left, view of the DuMi end station with collimating slits (1) and electrostatic lens (2) for beams from the 6.0 MV tandem. Scanner coils (3) and magnetic quadrupole triplet (4) are for ion beams from the 1.0 MV tandem. Middle, schematic presentation of the arrangement. Right, view of the main chamber interior. The Ge detector for PIGE is seen on the right (A), SDD detector for PIXE is viewing the sample from above (B), annular silicon detector is seen at the top (C), while another silicon detector seen on the left is used for NRA (D). Sample holder is positioned at the Piezo xyz stage (E), while at the bottom of the picture is seen detector for the direct and off-axis STIM (F). Behind the STIM detector is a Faraday cup, not visible in this view.

forward scattered particles. In addition, annular SDD x-ray detector with 4 segments of 15 mm^2 (PNDetector, Rococo 2), that will be mounted at the sidewise 90-degree port of the prechamber, will enable high spatial resolution PIXE measurements. Positioning of this detector at 3 mm distance from the sample will enable PIXE analysis with 1 sr solid angle. This detector is currently under the procurement.

2.2. Electromagnetic quadrupole triplet lens

The electromagnetic quadrupole triplet focusing system is positioned at the −10 degree beam line of the 1.0 MV Tandetron accelerator (see Fig. 1). Its initial aim was to release the pressure of increasing number of users and applications working with the old RBI microprobe system [12]. In addition, the number of techniques based on the ion microprobe was also increasing and a single universal system was not any more an option that can fulfil the best working conditions for all the techniques. Finally, the possibility to have two microbeams in one scattering chamber, which was feasible for this particular position in the accelerator laboratory, was offering new and exciting application possibilities.

The ion optical system begins with a remotely controlled object apertures produced by Technisches Büro Fischer (Mod. 3.2), which is positioned between the analysing and the switching magnet of the Tandetron accelerator. This aperture system is based on two sets of slits (for the x and y planes) where each slit consists of two tungsten cylinders, separated on one side by 150 μm, enabling fine tuning of the aperture dimensions continuously between 0 and 150 μm. The distance between the object aperture and the face of the first magnetic quadrupole lens is 538 cm. Before the lens itself, a collimating aperture system and magnetic scanner are installed as well.

The focusing lens is based on a set of three magnetic quadrupoles which can be connected in three different configurations (high and low excitation triplet and doublet). Each of the quadrupoles is made from one piece that is machined with a tolerance in the order of 20 μm. The quadrupole bore hole diameter is 11 mm, while its hyperbolic surface extends up to a diameter of 26 mm. The maximal magnetic field at the pole tip is measured to be 0.46 T. The quadrupole length is 70 mm while the quadrupole outer diameter is 18 cm. The typical focusing configuration used is classical high excitation Oxford triplet with CDC (converging, diverging, converging) polarization of the quadrupoles. Power supplies (TDK Lambda, GENH100-7.5) are powering the first two quadrupoles (polarized oppositely) and the final quadrupole, respectively. Unfortunately, the high excitation triplet cannot focus the highest

rigidity ions that 1.0 MV tandem accelerator can provide. In such a case only the first two lenses are polarized as a doublet. The characteristics of the focusing lens system are listed in the Table 1. System demagnifications for two different working distances (short and long) were calculated using the FANM software [13].

2.3. Electrostatic quadrupole quadruplet lens

The electrostatic quadrupole quadruplet lens focusing system is

Table 1
Characteristics and performance of the dual microprobe focusing system obtained by 2 MeV protons.

Magnetic quadrupole triplet	
Object slit to lens distance (cm)	538
Quadrupole bore hole (mm)	11
Quadrupole length (mm)	70
Triplet total length (mm)	300
Working distance – long focus (mm)	262
Demagnification × – long focus	36.8
Demagnification y – long focus	−16.6
Working distance – short focus (mm)	70
Demagnification × – short focus	147.5
Demagnification y – short focus	−33.2
Long focus spot size (x,y) – low current* (μm)	0.46, 0.60
Long focus spot size (x,y) – high current** (μm)	3.01, 3.70.
Short focus spot size (x,y) – low current* (μm)	0.12, 0.34
Short focus spot size (x,y) – high current** (μm)	0.66, 1.28
Electrostatic quadrupole quadruplet	
Object slit to lens distance (cm)	350
Quadrupole bore hole (mm)	6.1
Quadruplet system length (mm)	326
Working distance – long focus (mm)	363
Demagnification***	16.1
Minimum spot size (x,y) – high current** (μm)	7.5, 15,0

*In the low current operation mode, the object aperture was set to approximately 5 × 5 μm², while the collimator aperture was set to approximately 20 × 20 μm². This resulted in beam current of the 0.2 fA order.

**For the high current mode, for both magnetic triplet and electrostatic quadruplet, object apertures were set to 50 × 50 μm while collimator slits were set to approximately 250 × 250 μm². This resulted in currents of the 10 pA order for proton beams obtained by either of two accelerators.

***Demagnification value for the electrostatic lens is taken from ref. [15], as calculated for object to lens distance 527 cm and lens to image distance of 326 mm.

positioned at the +30 degree beam line of the 6.0 MV tandem accelerator (see Fig. 1). Its main aim is to use primarily heavy ion beams, for irradiation / implantation purposes. Due to higher acceleration voltages of this larger accelerator, heavy ions will have similar range in target material as light ions provided by the smaller accelerator. This can often be a good advantage, in particular for dual beam irradiation that can simulate high radiation fields such as those found in fusion reactors. In that case, for example, when tests of steel radiation hardness will be needed, Fe ions will simulate neutron damage assuming that elastic scattering of neutrons on Fe nuclei is the primary cause of radiation damage. For the Fe ions of 20 MeV energy (range in steel 3 μm), similar depth profile of produced vacancies will have 2 MeV He ions. Helium and hydrogen are expected to be created in fusion reactors as a product of neutron transmutation of iron [10]. Irradiation by dual microbeam may have additional advantage when compared to the broad beam irradiation, when focused beam is scanned over the small surfaces, achieving locally (at small areas) very high fluences. Also, raster scanning can enable very homogeneous irradiation. However, it has to be noted that effects of irradiation by scanned focused beam may be different in some materials from those done with unfocused beam [14].

The ion optical system of this electrostatic microprobe begins with a manually controlled object aperture system which is placed between the analysing and switching magnets of the tandem Van de Graaff accelerator. This aperture system is based on x and y slits that are each made of two tungsten cylinders that form a wedge-shaped beam opening of size between 0 and 1 mm. In order to minimize the influence of switching magnet, which is single focusing and thus has some focusing action in horizontal plane, another horizontal collimating slit is installed at the exit port of the switching magnet to decrease the beam divergence. The final collimating slits are positioned just in front of the electrostatic lens and are independently adjusted (up, down, left, right).

The electrostatic quadruplet lens is produced by HVEE [15]. Distance between the quadrupole surfaces (bore hole) is 6.1 mm while the working distance for the long focus position is 35 cm. The space dedicated for a short focus mode of operation is reserved for the installation of electrostatic scanner, but can be used in future with working distance of 16 cm. The most important parameters of the lens are summarized in Table 1. Currently, imaging can be performed only by scanning the sample using the Piezo stage.

2.4. Data acquisition and microprobe control

Data acquisition (DAQ) system based on the SPECTOR software system has been in constant development since its first version has been installed at the first RBI microprobe back in the nineties [16–18]. Gradually, along with several changes in hardware, more specifically the move to FPGA technology, many other options have been implemented into SPECTOR. The most important, in the contest of this work, is the beam scanning control, the possibility to scan the sample, either in specific area (x,y) or by angular control (θ,φ) for channelling. The DAQ system can also control beam pulsing, which is important for switching on and off two microbeams which can be dependent or independent. Also, beam pulsing is important for timing measurements (e.g. the TOF options of MeV SIMS), while SPECTOR also controls a beam chopper important for indirect fluence measurements. The latest developments, important for the DuMi system are focused on a more integrated environment achieved by integrating the DAQ system with the experimental physics and industrial control system (EPICS) used to control the accelerators. This allows the microprobe acquisition system to automatically control various aspects of the accelerator system, such as the beam line values and Faraday cups to precisely monitor the beam current in order to achieve accurate and reproducible irradiation doses. Furthermore, the integration of the DAQ system with EPICS allows for important accelerator and experiment setup parameters to be automatically logged and saved as metadata with the acquired spectra.

3. Results and discussion

3.1. Performance tests

Spatial resolution tests for both focusing systems have been performed for 2 MeV protons. As a test sample a micromachined Ni resolution standard produced at NUS [19] has been used (Fig. 3). It has regions with different grid spacings and therefore can serve for tests of large range of spatial resolutions. Also, by SEM imaging it was confirmed that its grid edges are much better defined comparing to standard Cu grids used in electron microscopy, which are not appropriate for resolutions reaching 100 nm. For the electromagnetic quadrupole triplet lens, resolution tests have been performed for both short and long focus positions and for low current and high current operation modes. Typical object and collimator slit openings are given in the table. Low current modes were tested by STIM detector, while for the high current mode either PIXE (for long focus) or off-axis STIM (for short focus) have been employed. Images shown in Fig. 3 present counts in the energy windows that correspond to ions passing through Ni grid. Results of all characteristics and tested performances are summarized in Table 1. Spatial resolutions were obtained by fitting the error function over the edges of grid in x and y dimensions. As can be seen, the best spatial resolution has been obtained for a short focus position and low current mode operation of the triplet lens. Spatial resolution of 0.12 μm for x and 0.34 μm for y dimension has been obtained. STIM image of the nickel resolution standard as well as the best fit of over the edge are presented in Fig. 3.

Concerning the performance of the electrostatic quadruplet, results are within the expectations published in [15]. Although system was not aimed for high resolution experiments, performance test in high current mode has shown capability to reach focus of sizes of the 10 μm range (Fig. 4).

3.2. Applications – single microbeam

During the first year of routine operation of the magnetic quadrupole triplet system of the DuMi end station, several experiments have been performed with applications in different fields, i.e. ion beam analysis applications as well as irradiation of materials.

Regarding the application of ion beam analysis techniques, several experimental sessions during the recent year have been devoted to analytical tasks associated to Eurofusion project and also to users' projects of the CERIC-ERIC consortium [20]. Synergies of PIXE, RBS and STIM (or off-axis STIM) techniques were exploited to characterize archaeological and biological samples as well as to analyze samples of interest to fusion. In the former, in the context of the development of a new analytical protocol for residues characterization in the field of Paleolithic studies, red residues coming from lithic artefacts retrieved from the Upper Palaeolithic stratigraphic sequence of Grotta Paglicci (Apulia, Italy) were studied [21]. Different areas of interest on samples that have been measured previously by means of LEXRF microscopy at Elettra Sincrotrone Trieste (Italy) facility, were analysed by PIXE to obtain complementary information. Another application of PIXE imaging, this time done in combination with off-axis STIM, also accomplished through the CERIC-ERIC users' access program, is the analysis of mice and human lung tissue [22]. The main purpose of this project is establishment of a correlative analysis pipeline for lung fibrosis characterization. Finally, W tiles covered with gold marker spots after exposure to H-mode plasmas of ASDEX upgrade, were studied in the DuMi setup by means of micro-RBS and PIXE with a 2 MeV proton beam. In this way, Au particles were identified and also, quantitative elemental profiles as a function from the distance around (OSP) of the AUG divertor were obtained [23].

In respect to the ion irradiation of materials, two different applications have been performed. The existence of a chopper system, explained earlier, enable reliable measurement of fluences delivered to the microscopic sample areas, which were determined by the microbeam
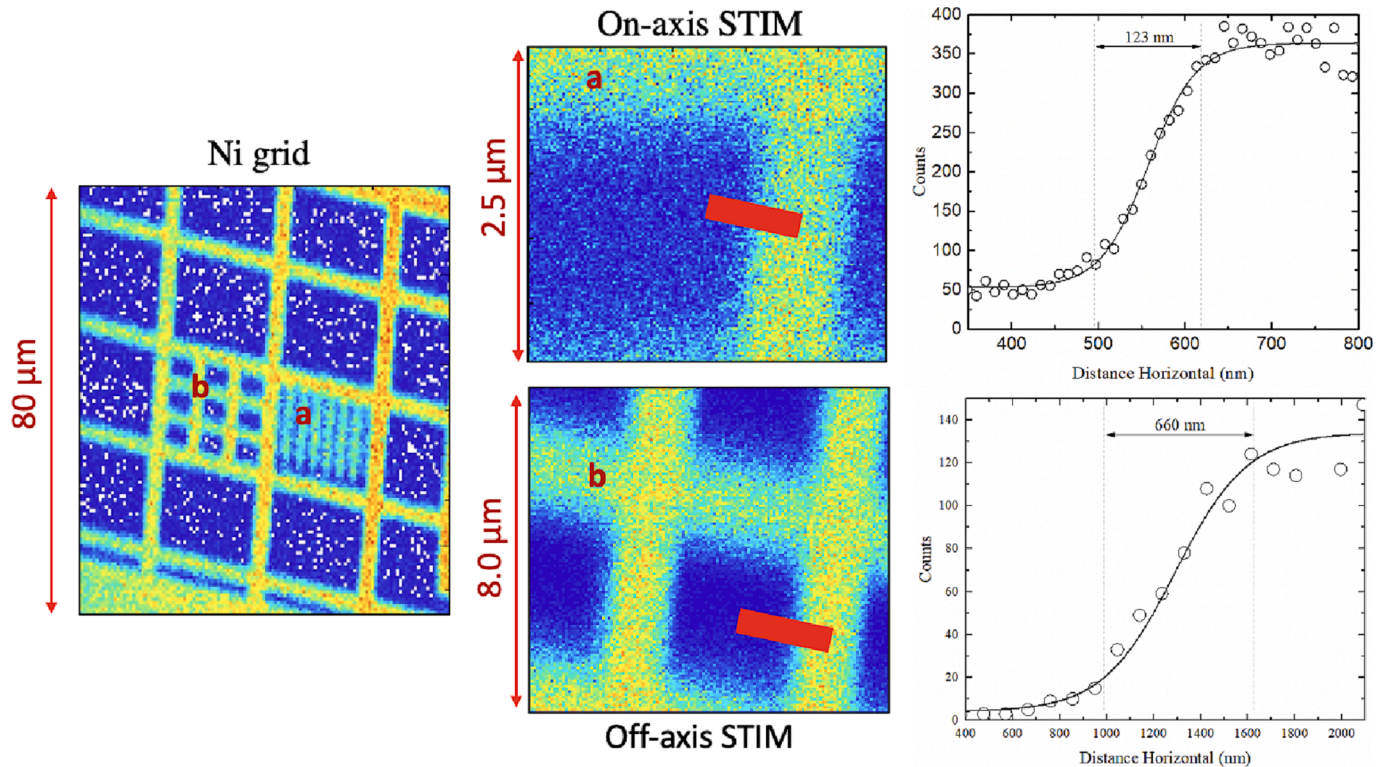
Fig. 3. Resolution test performed at the short focus position, using 2 MeV proton microbeam. Both, STIM and off-axis STIM images, correspond to summed events in the energy window of protons transmitted through the Ni grid. Test grid consists of regions with different spacings as seen on left. Images corresponding to the short focus position are shown in the middle, with low current (a, STIM) and high current (b, off-axis STIM) operation modes. Corresponding error function fits along the horizontal grid edge (indicated by bars) were shown for low current (upper right) and high current (lower right) modes. Results are summarized in Table 1.

scanning parameters. This was employed for the evaluation of response of glass dosimeters to proton irradiation, and also for the fabrication of color centres in diamond. In the former, FD-7 radio-photoluminescent glass dosimeters were exposed to protons with energies up to 2 MeV. Aiming to study the corresponding dose response, the dosimeters of 1×1 mm^2 area were exposed to different proton fluences in the range 10^7–10^{10}p/cm^2. Their corresponding RPL (Radiophotoluminescence) signals were then measured at the RBI Dosimetry Laboratory with a FGD-202 reader [24,25]. Within the framework of the RADIATE project, single-photon emitters based on germanium-vacancy (GeV) defects were fabricated by Ge ions being implanted into the CVD-grown single-crystal diamond. In order to reach implantation depths of around 1 μm, 3 MeV ions were scanned over 200×200 μm^2 area in the range of fluences between 1 and 3×10^{10} ions/cm^2 [26]. For the aforementioned irradiations, openings of both object and collimator slits were reduced until the ion currents between 10^3 and 10^5 ions/s were obtained. These were monitored by pin diode that periodically intercepts the microbeam.

3.3. Applications – dual microbeam

Since the electrostatic quadruplet has been installed just recently, only two applications that utilize simultaneously two microbeams have been tested. The first one is rather simple, but clearly illustrates the advantage of the dual microbeam irradiation – probing approach. It is related to the surface deposition of hydrocarbons during irradiation. This effect is particularly important to consider when heavy ions of small range are used to irradiate materials. If significant deposition of hydrocarbons occurs, the range of ions will be changed as well, influencing the final depth distribution of implanted ions and therefore corresponding damage profiles. In order to demonstrate that deposition of hydrocarbons can be monitored in situ, we have used irradiation of thin Al foil by 6 MeV Si ions. Deposition of C and O on Al film has been

monitored by RBS using proton beam of 2 MeV. As it is seen from Fig. 5, the increase of the RBS C peak intensity, normalized to Al peak, can be clearly observed. Although Si ions cannot backscatter from such a target, small low energy background can be noticed at low energy side of RBS spectra. This was caused most likely due to rare multiple scattering events, and/or Si ion backscattering from heavier impurities in the Al foil.

The second application tested was the on-line monitoring of the ion beam induced damage introduced in crystalline materials. Particularly interesting are studies of dynamic annealing process that take place for example in Si and SiC. This includes dependence of ion beam induced radiation damage on temperature and irradiation dose rate. These processes have been earlier studied by pulsed beam irradiation and subsequent RBS channelling (RBS/c) analysis [27,28]. However, performance of ion beam irradiation and ion beam probing simultaneously by two beams can certainly offer a new insight into these processes. To investigate if such study consisting of damaging and RBS/c probing can be performed with focused ion beams, a proof-of-concept experiment was designed. First, the sample was irradiated with a 750 keV Cl ions in several well defined regions with 50×50 μm^2 areas. This was followed by a RBS/c experiment using 1 MeV proton microbeam. The sample was mounted on a Piezo stage with (θ, ϕ) scanning capability, positioned into the long-focus position of the main chamber. After finding the channelling direction, the sample rotation was fixed, and spatially resolved RBS/c maps were recorded by raster scanning the beam. One of these maps, as well as RBS/c spectra, are shown in Fig. 5. Damaged zones are clearly resolved, demonstrating that such channelling microscopy setup is successful in quantifying effects of radiation damage. To increase channelling contrast, the probing beam was focused using only the first two quadrupole lenses connected as doublet, resulting in lower demagnification action. Results show, that this technique can be used for the quantitative studies of dynamic annealing by simultaneous use of
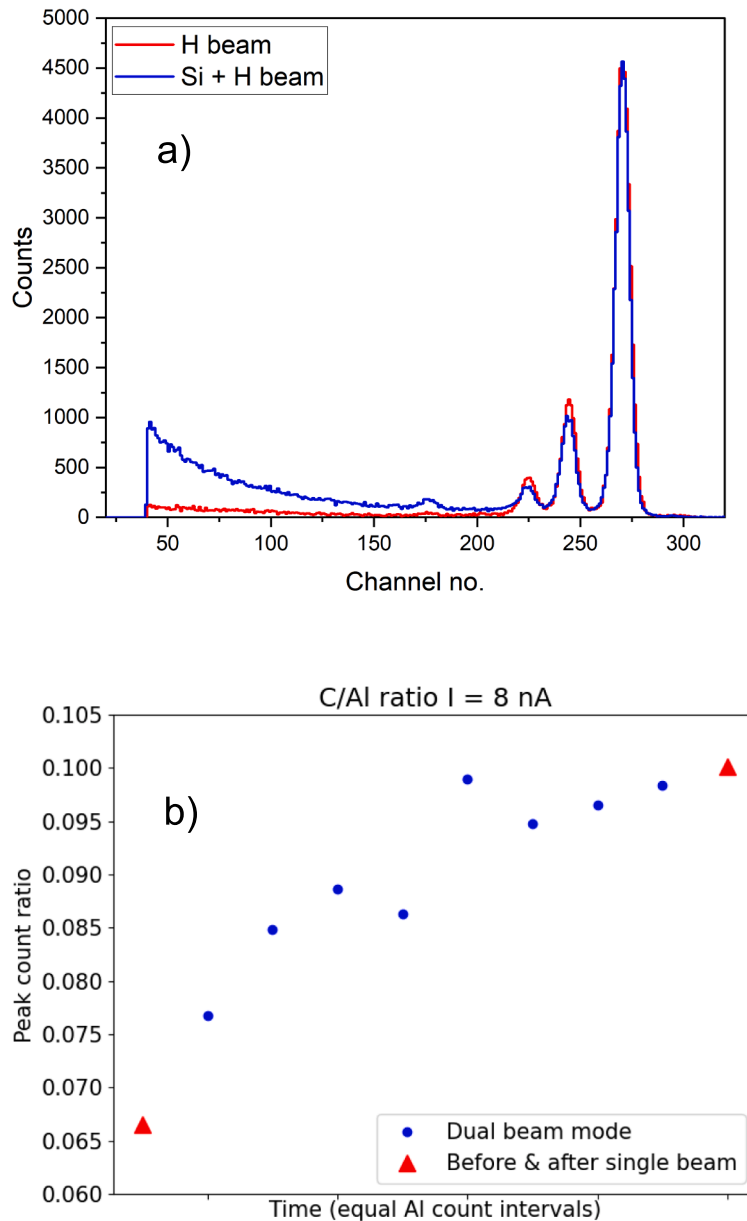
Fig. 4. (a) Typical RBS spectra of the Al foil obtained by 2 MeV protons in single beam mode (only protons) and dual beam mode (both protons and Si ions). (b) Evolution of the carbon thickness monitored by RBS during the one of the sequences of irradiation with 6 MeV Si ions of the same region.

two ion beams. Irradiation beam should be heavier than elements that exist in irradiated materials to avoid backscattering. In the case of DuMi setup, the probing beam could be either protons or He ions.

4. Conclusions

A new experimental setup consisting of the two independent ion microprobes, that can be also used simultaneously, has been explained. High resolution ion microbeam, provided by smaller tandem accelerator, is focused by in-house made magnetic quadrupole triplet. It is mainly applied for materials characterization (PIXE, RBS, NRA, STIM, IBIC) with spatial resolution down to 300 nm obtained for low current operation mode (STIM). Electrostatic quadrupole quadruplet is used to focus higher energy protons for NRA and PIGE as well as for irradiation

by heavy ions. In this case ion beam is supplied by larger tandem accelerator. In that sense each of the microbeam systems can be used independently. However, the main strength of this unique system comes from the fact that the two ion microbeams can be used simultaneously. This is in particular appealing for experiments based on damaging/ probing concept, where one microbeam is used to create changes in irradiated sample while the other is used to detect these changes. Result of one simple experiment (hydrocarbon deposition) based on this approach has been presented. In addition, successful proof of concept has been performed for in situ study of damaging process in crystalline materials using simultaneous RBS channelling. Although the system has been planned mostly for studies of electronic materials and materials of importance for fusion, application possibilities of the system could be much wider.
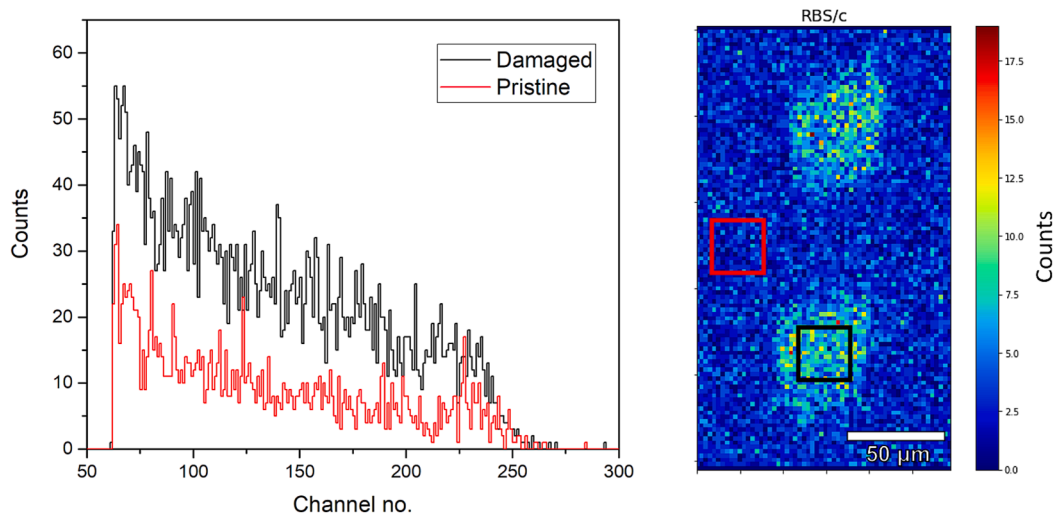
Fig. 5. RBS/c spectra obtained by 1 MeV protons shown on left are extracted from the two regions indicated in RBS/c intensity map shown on right. Higher intensity regions correspond to $50 \times 50\ \mu m^2$ areas irradiated by 650 keV Cl ions due to de-channelling caused by radiation damage.

Declaration of Competing Interest

The authors declare that they have no known competing financial interests or personal relationships that could have appeared to influence the work reported in this paper.

Acknowledgements

References

[1] J.A. Hinks, A review of transmission electron microscopes with in situ ion irradiation, Nucl. Instr. Meth. B 267 (2009) 3652–3662.

[2] K. Hattar, D.C. Bufford, D.L. Buller, Concurrent in situ ion irradiation transmission electron microscope, Nucl. Instr. Meth. B 338 (2014) 56–65.

[3] A. Canizarès, G. Guimbretière, Y.A. Tobon, N. Raimboux, R. Omnée, M. Perdicakis, B. Muzeau, E. Leoni, M.S. Alam, E. Mendes, D. Simon, G. Matzen, C. Corbel, M. F. Barthe, P. Simon, In situ Raman monitoring of materials under irradiation: study of uranium dioxide alteration by water radiolysis, J. Raman Spectrosc. 43 (2012) 1492–1497.

[4] R. Brunetto, G.A. Baratta, G. Strazzulla, Amorphization of diamond by ion irradiation: a Raman study, J. Phys.: Conf. Ser. 6 (2005) 120–125.

[5] V.A. Skuratov, K.J. Gun, J. Stano, D.L. Zagorski, In situ luminescence as monitor of radiation damage under swift heavy ion irradiation, Nucl. Instr. Meth. B 245 (2006) 194–200.

[6] N. Marković, Z. Siketić, D. Cosic, H.K. Jung, N.H. Lee, W.T. Han, M. Jakšić, Ion beam induced luminescence (IBIL) system for imaging of radiation-induced changes in materials, Nucl. Instr. Meth. B 343 (2015) 167–172.

[7] L. Beck, Y. Serruys, S. Miro, P. Trocellier, E. Bordas, F. Leprêtre, D. Bachiller-Perea, Ion irradiation and radiation effect characterization at the JANNUS-Saclay triple beam facility, J. Mat. Res. 30 (2015) 1183–1194.

[8] J.R. Kaschny, R. Kögler, H. Tyrrof, W. Bürger, F. Eichhorn, A. Mücklich, C. Serre, W. Skorupa, Facility for simultaneous dual-beam ion implantation, Nucl. Instr. Meth., A 551 (2005) 200–207.

[9] S. Hamada, Y. Miwa, D. Yamaki, Y. Katano, T. Nakazawa, K. Noda, Development of a triple beam irradiation facility, J. Nucl. Mat. 8 (1998) 383–387.

[10] J. Knaster, A. Moeslang, T. Muroga, Materials research for fusion, Nat. Phys. 12 (5) (2016) 424–434.

[11] T. Tadić, personal communication.

[12] M. Jakšić, I.B. Radović, M. Bogovac, V. Desnica, S. Fazinić, M. Karlušić, Z. Medunić, H. Muto, Ž. Pastuović, Z. Siketić, New capabilities of the Zagreb ion microbeam system, Nucl. Instr. Meth., B 260 (2007) 114–118.

[13] Y. Dou, J.A. van Kan, FANM: A software for focus and aberrations of nuclear microprobe, Ultramicroscopy 220 (2021), 113163.

[14] J.G. Gigax, E. Aydogan, T. Chen, D. Chen, L. Shao, Y. Wu, W.Y. Lo, Y. Yang, F. A. Garner, The influence of ion beam rastering on the swelling of self-ion irradiated pure iron at 450 C, J. Nucl. Mater. 465 (2015) 343–348.

[15] N.C. Podaru, F.L. Van De Hoef, A. Gottdang, D.J.W. Mous, Design and performance of the HVE electrostatic nuclear microprobe, Nucl. Instr. Meth., B 306 (2013) 25–28.

[16] M. Bogovac, I. Bogdanović, S. Fazinić, M. Jakšić, L. Kukec, W. Wilhelm, Data acquisition and scan control system for nuclear microprobe and other multiparameter experiments, Nucl. Instr. Meth. B 89 (1994) 219–222.

[17] M. Bogovac, M. Jakšić, D. Wegrzynek, A. Markowicz, Digital pulse processor for ion beam microprobe imaging, Nucl. Instr. Meth. B 267 (2009) 2073–2076.

[18] D. Cosic, M. Bogovac, M. Jakšić, Data acquisition and control system for an evolving nuclear microprobe, Nucl. Instr. Meth. B 451 (2019) 122–126.

[19] F. Watt, I. Rajta, J.A. van Kan, A.A. Bettiol, T. Osipowicz, Proton beam micromachined resolution standards for nuclear microprobes, Nucl. Instr. Meth. B 190 (2002) 306–311.

[20] https://www.ceric-eric.eu.

[21] C. Dominici, C. Stani, M. Rossini, L. Vaccari, SR-FTIR microscopy for the study of residues on Palaeolithic stone tools: looking for a methodological protocol, J. Phys.: Conf. Ser. 2204 (2022), 012050.

[22] Lorenzo D'Amico, personal communication.

[23] A. Lahtinen, A. Hakola, J. Likonen, M. Balden, K. Krieger, S. Gouasmia, I. Bogdanovic Radovic, G. Provatas, M. Kelemen, S. Markelj, M. Pedroni, A. Uccello, E. Vassallo, D. Dellasega, M. Passoni, Influence of surface morphology on erosion of plasma-facing components in H-mode plasmas of ASDEX Upgrade, Nucl. Mater. Energy 33 (2022), 101266.

[24] T. Yamamoto, R.P.L. Dosimetry, Principles and Applications, AIP Conf. Proc. 1345 (2011) 217–230.

[25] M. Majer, I. Ambrožová, M. Davídková, M. De Saint-Hubert, M. Kasabašić, Ž. Knežević, R. Kopeć, D. Krzempek, K. Krzempek, S. Miljanić, N. Mojżeszek, I. Veršić, L. Stolarczyk, R.M. Harrison, P. Olko, Out-of-field doses in pediatric craniospinal irradiations with 3D-CRT, VMAT, and scanning proton radiotherapy: a phantom study, Med. Phys. 49 (2022) 2672–2683.

[26] J. Christinck, personal communication.

[27] M.T. Myers, S. Charnvanichborikarn, L. Shao, S.O. Kucheyev, Pulsed ion beam measurement of the time constant of dynamic annealing in Si, Phys. Rev. Lett. 109 (2012) 095502.

[28] J.B. Wallace, L.B. Bayu Aji, L. Shao, S.O. Kucheyev, Time constant of defect re-laxation in ion-irradiated 3C-SiC, Appl. Phys. Lett. 106 (2015), 202102.